Electronic Supplementary Material (ESI) for New Journal of Chemistry.
This journal is © The Royal Society of Chemistry and the Centre National de la Recherche Scientifique 2023

Supporting information

Study on the photocatalytic hydrogen production of covalent triazine framework regulated by different π bridges

Xiangyu Li[a,b], Minghui Chen[a,b], Quan Shi[a,b], Ji Xiong[a,b], Ting Li[a,b], Yu Jiang[a,b], Prof. Yaqing Feng[a,b], Prof. Bao Zhang[a,b,c,]*

a. School of Chemical Engineering and Technology, Tianjin University, Tianjin 300350, China.

E-mail: baozhang@tju.edu.cn

b. Guangdong Laboratory of Chemistry and Fine Chemical Industry Jieyang Center, Guangdong Province, 522000, P. R. China

c. Haihe Laboratory of Sustainable Chemical Transformations, Tianjin 300192, China.

Corresponding authors:

baozhang@tju.edu.cn (B. Zhang)

1. Experimental and characterization details

1.1 Chemicals and reagents

All chemicals and reagents were used as received from commercial sources without further purification. N, N-dimethylformamide (DMF), Dimethyl sulfoxide (DMSO), p-benzamidine dihydrochloride, Nafion perfluorinated resin solution were purchased from Aladdin industrial corporation, Shanghai, China. K_2CO_3 was purchased from Kmart chemical technology limited company, Tianjin, China. Cs_2CO_3, 1,3,5-tris(4,4,5,5-tetramethyl-1,3,2-dioxaborolan-2-yl) benzene, $Pd(PPh_3)_4$, 1,3,5-Tris(p-formylphenyl)benzene and 5,5',5''-(Benzene-1,3,5-triyl)tris(thiophene-2-carbaldehyde) were purchased from Shanghai bide Pharmaceutical Technology Co. Dichloromethane, acetone, hydrochloric acid, saturated sodium bicarbonate, anhydrous sodium sulfate, petroleum ether, ethanol, Silicone (200-300 mesh) were purchased from Jiangtian chemical technology limited company, Tianjin, China.

1.2 Characterization methods

Liquid 1D ^{1}H NMR spectra of all monomers were recorded on a Bruker AVANCE IIITM HD 400 MHz NanoBAY. And 600 M solid-state ^{13}C Nuclear Magnetic Resonance (^{13}C NMR) spectra were measured on the JEOL JNM ECZ600R. Powder X ray diffraction (PXRD) data were collected on Rigaku Smartlab8KW using Cu Kα radiation at 40 kV,40 mA power. Fourier-transform infrared (FT-IR) spectra was recorded on Nicolet6700 instrument (600-3500 cm^{-1}region). The Brunauer-Emmett-Teller (BET) surface areas were measured by nitrogen adsorption and desorption at 77 K using Autosorb-iQ2-MP and the samples were activated at 100 °C for 8 h under vacuum before analysis. Pore size distributions and pore volumes were derived from the adsorption branches of the isotherms using the density functional theory (DFT) pore mode. A Field

Emission Scanning Electron Microscope (FE-SEM) images were obtained with a Regulus 8100 electron microscope (Japan, Hitachi Limited). High-resolution Transmission Electron Microscopies (HR-TEM) and energy dispersive spectroscopy (EDS) were performed using JEOL model JEM-F200. The X-ray photoelectron spectroscopy (XPS) analysis was obtained by ESCALAB 250xi, Thermo Scientific. UV-Visible diffuse reflectance spectra (DRS) were obtained by Lambda 750, Perkin Elmer with an integrating sphere mode. The steady photoluminescence(PL) data was measured by FLS1000 fluorescence spectrometer in the solid state. Electrochemical properties of the material frameworks were measured through a three-electrode system in an electrochemical workstation with a brand of CHI66, Chenhua. For these measurements, 5 mg CTFs was dispersed into the mixed solvent of 1 mL ethanol and 0.2 mL 5wt% Nafion aqueous solution by ultrasonic 60 min. After that, 20 μL suspension was deposited onto clean Φ3 GCE as the working electrode. And the Ag/AgCl electrode worked as the reference electrode and Pt flake was acted as the counter electrode. 0.2 M Na_2SO_4 aqueous solution acted as electrolyte during the measurements. The photocatalytic performance was recorded by Labsolar6A, Perfectlight. The production of H_2 was detected by an online gas chromatograph (TCD detector, N_2 carrier, 5Å molecular sieve column) at given times intervals. The light source was a 300 W xenon lamp (Perfectlight, PLS-SXE300 + /UV) simulated AM 1.5 G illumination.

2. Preparation procedures

Synthesis of BenP-CHO((1,3,5-tris(4',4'',4'''-formylpyridine) benzene)

The monomer was synthesized according to the previously literature[1]. A mixture of 1,3,5-tris(4,4,5,5-tetramethyl-1,3,2-dioxaborolan-2-yl) benzene (680 mg, 1.5 mmol), 5-bromo-2-pyridinecarboxaldehyde (1.25 mg, 6.7 mmol), K_2CO_3 (3 g, 22 mmol), $Pd(PPh_3)_4$ (516.9 mg, 0.44 mmol) in anhydrous DMF (100 mL) was degassed and stirred under N_2 atmosphere at 90 ℃ for 24h. The solvent was removed under reduced pressure and the solid residue triturated with water, collected by filtration and washed with water (3×10 ml), hot diethyl ether (2×10 ml) and hot hexane (2× 10 ml). The dried solid was triturated with CH_2Cl_2 and collected again. The resulting product was redissolved in hot $CHCl_3$, the insoluble materials filtered off and Et_2O added to the filtrate to precipitate out pure product A as a pale-yellow solid (230 mg, 40%). ^{1}H NMR (600 MHz,) δ 10.15 (s, 1H), 9.11 (s, 1H), 8.17 (d, 1H), 8.11 (d, 1H), 7.94 (s, 1H).

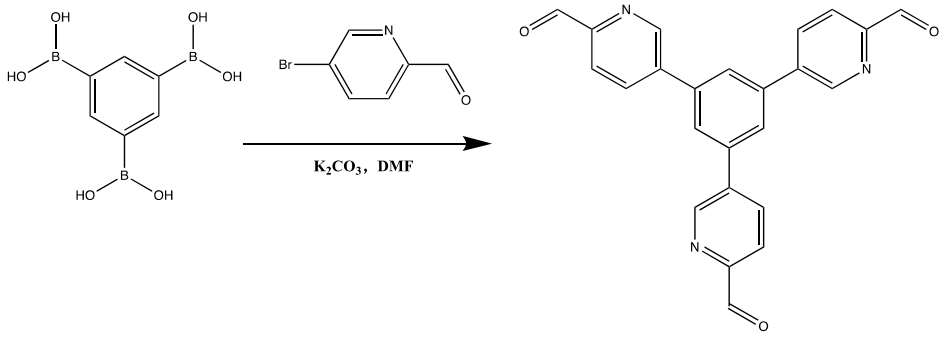

Figure S1. Synthetic route of BenP-CHO

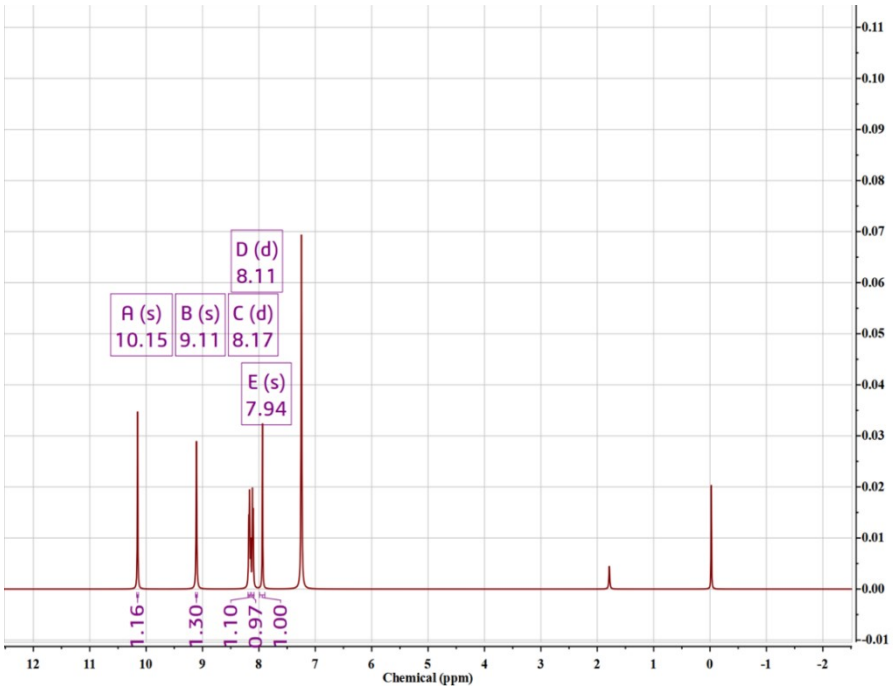

Figure S2. The ^{1}H NMR spectra of BenP-CHO in $CDCl_3$.

3. Characterization

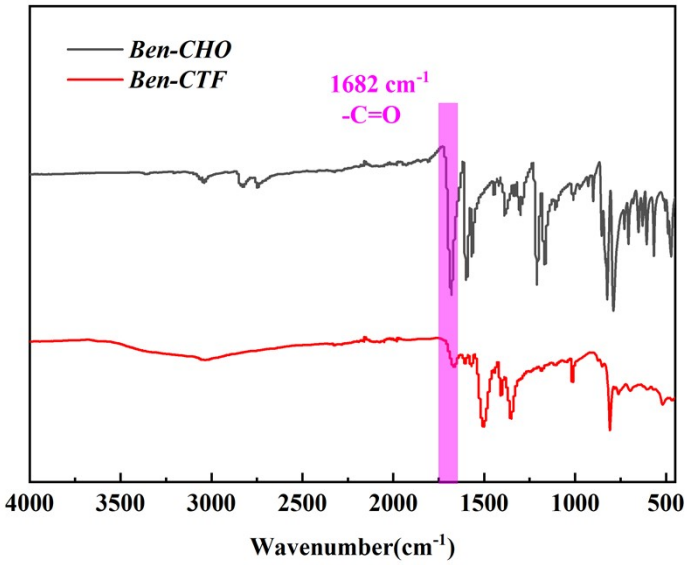

Figure S3. FT-IR spectrum of Ben-CTF with starting molecules (Ben-CHO).

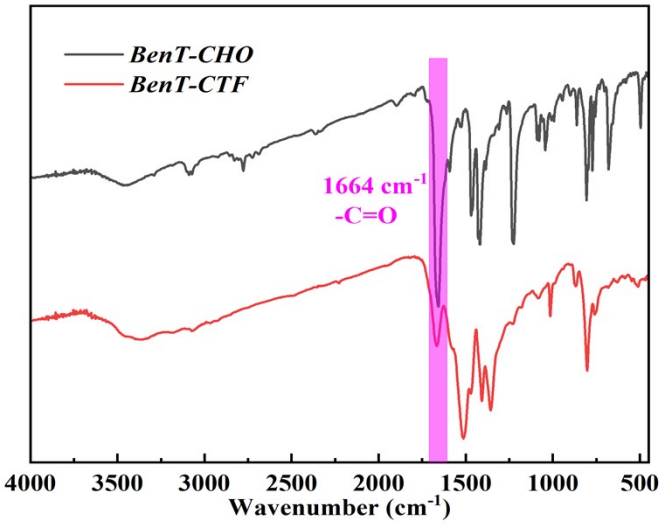

Figure S4. FT-IR spectrum of BenT-CTF with starting molecules (BenT-CHO).

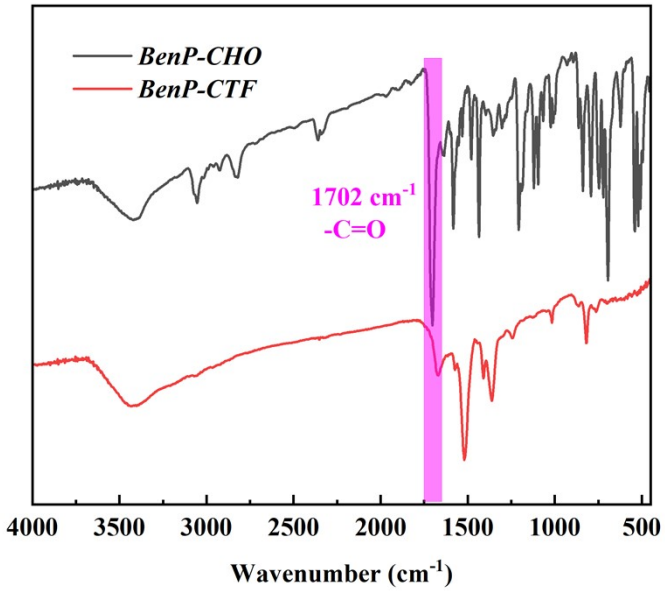

Figure S5. FT-IR spectrum of BenP-CTF with starting molecules (BenP-CHO).

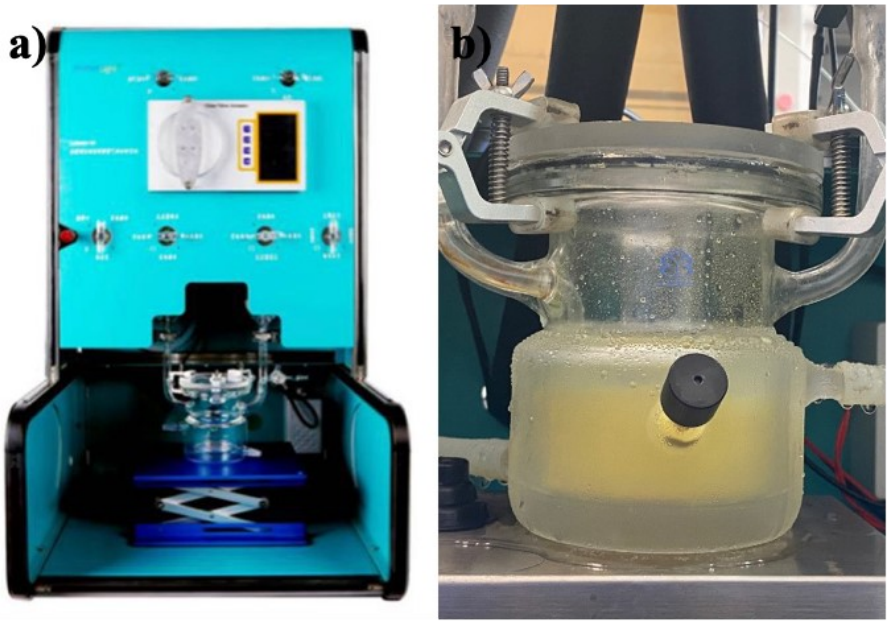

Figure S6. (a) Photograph of the photocatalytic on-line analytical system (Labsolar-6A, PerfectLight); (b) Quartz reactor with condensate.

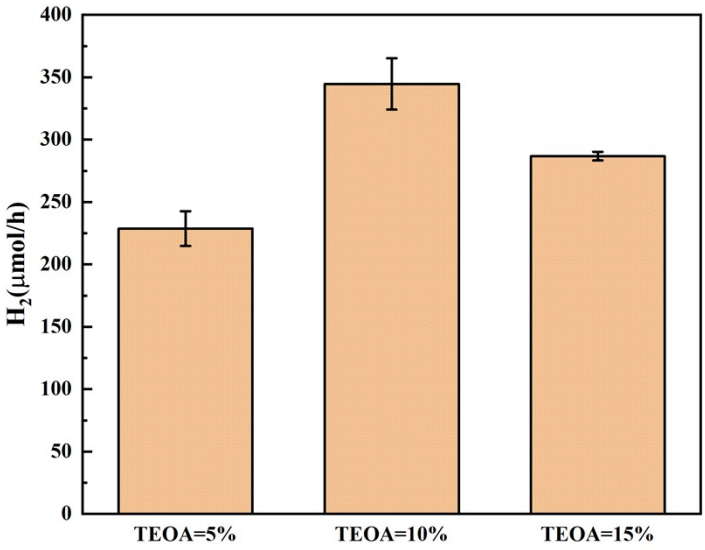

Figure S7. Photocatalytic performance of BenP-CTF in different amount of TEOA.

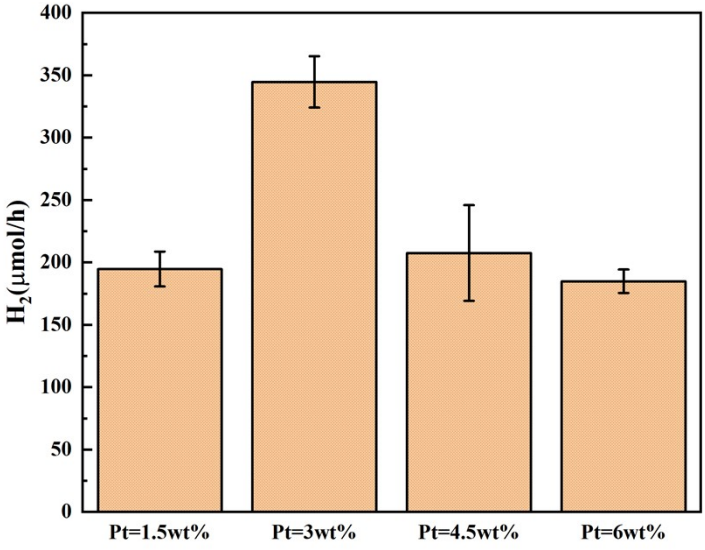

Figure S8. Photocatalytic performance of BenP-CTF in different amount of Pt.

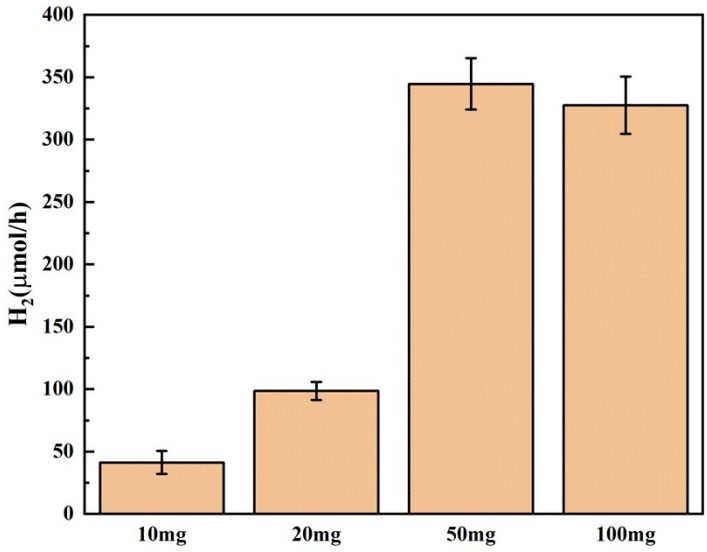

Figure S9. Photocatalytic performance of BenP-CTF in different amount of CTF.

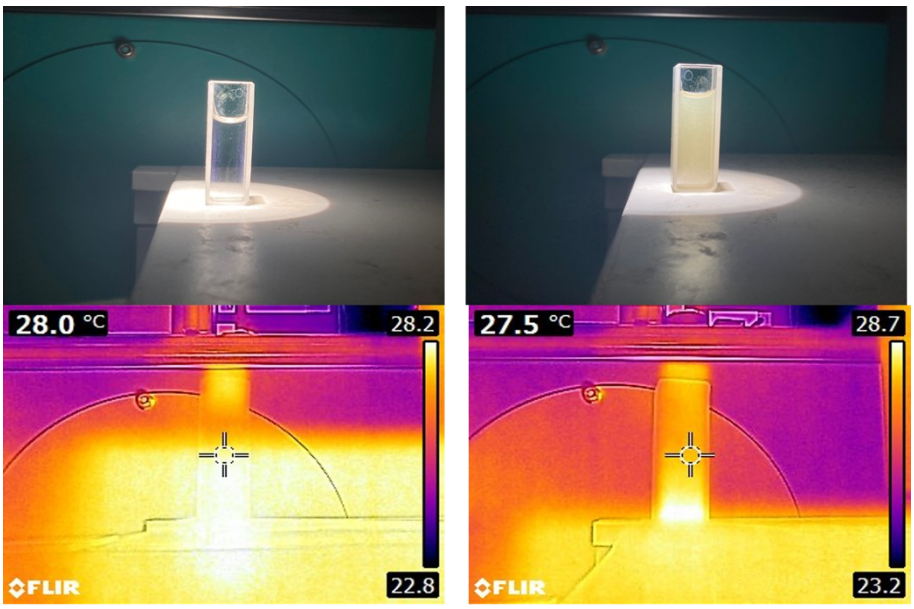

Figure S10. Photothermal experiment for BenP-CTF under a 300 W xenon lamp simulated AM 1.5 G illumination.

As shown in the Figure S10, after 1h, 10% aqueous solution of TEOA containing BenP-CTF under a 300 W xenon lamp simulated AM 1.5 G illumination did not exhibit an increased temperature compared to that without BenP-CTF under the same conditions.

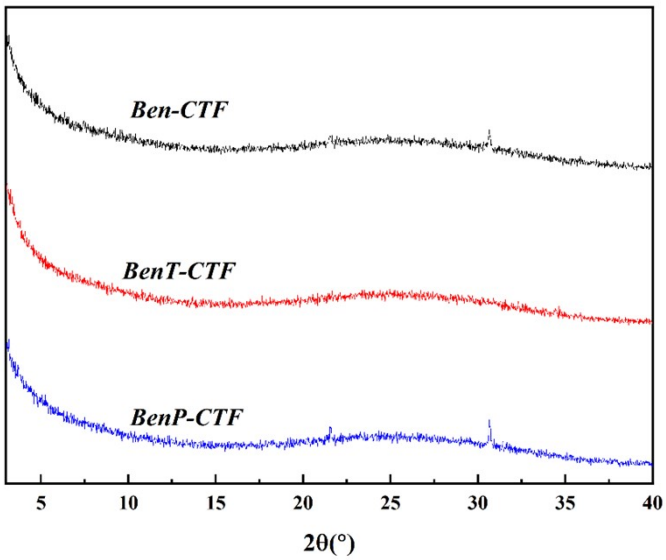

Figure S11. PXRD spectrum of Ben-CTF, BenT-CTF, and BenP-CTF.

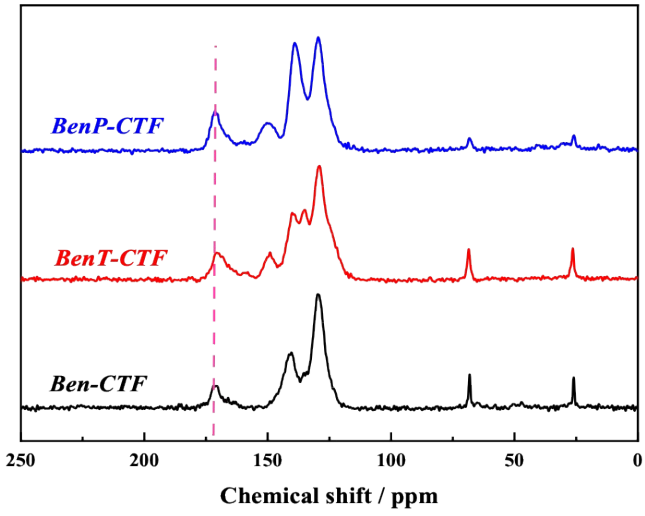

Figure S12. The full solid-state 13C NMR spectra of all final CTFs.

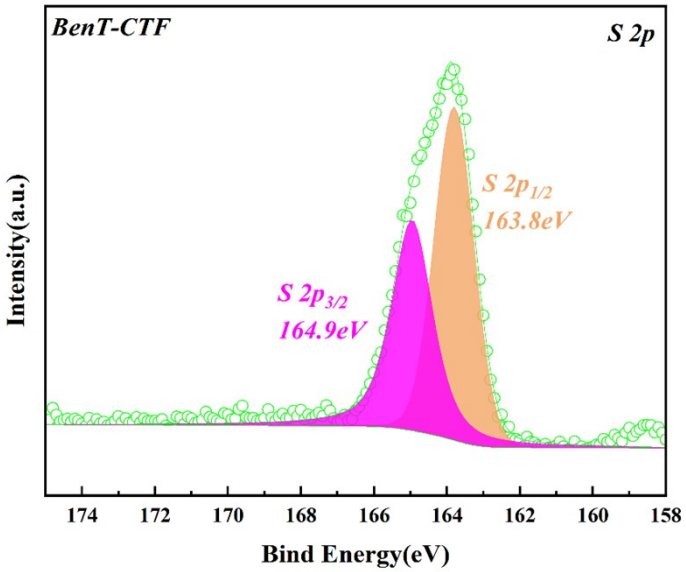

Figure S13. High-resolution XPS S 2p spectra of BenT-CTF.

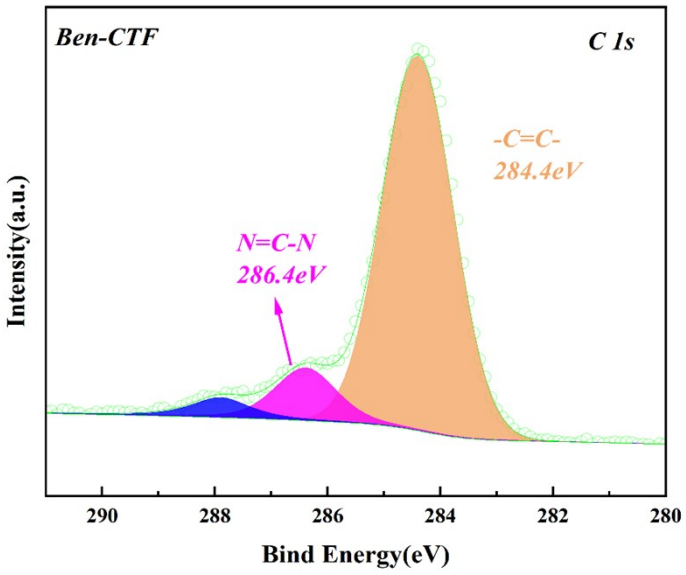

Figure S14. High-resolution XPS C 1s spectra of Ben-CTF.

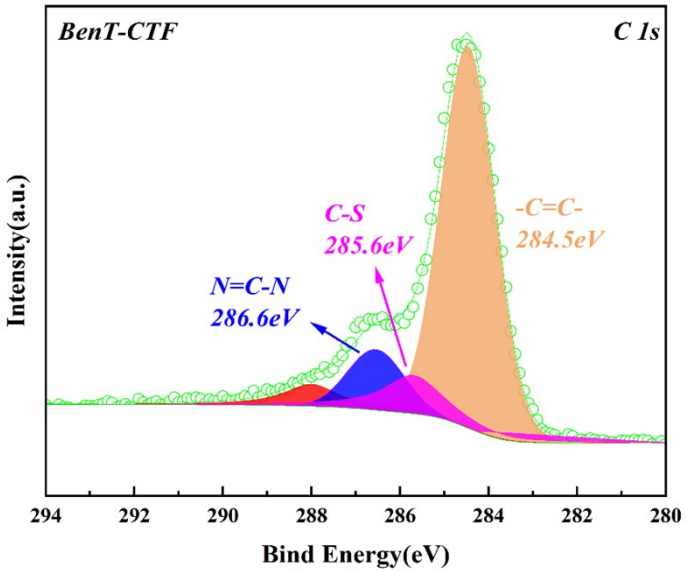

Figure S15. High-resolution XPS C 1s spectra of BenT-CTF.

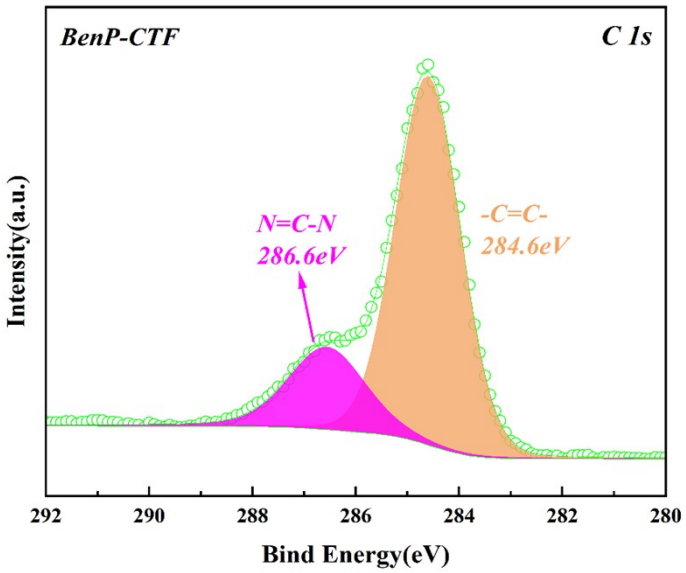

Figure S16. High-resolution XPS C 1s spectra of BenP-CTF

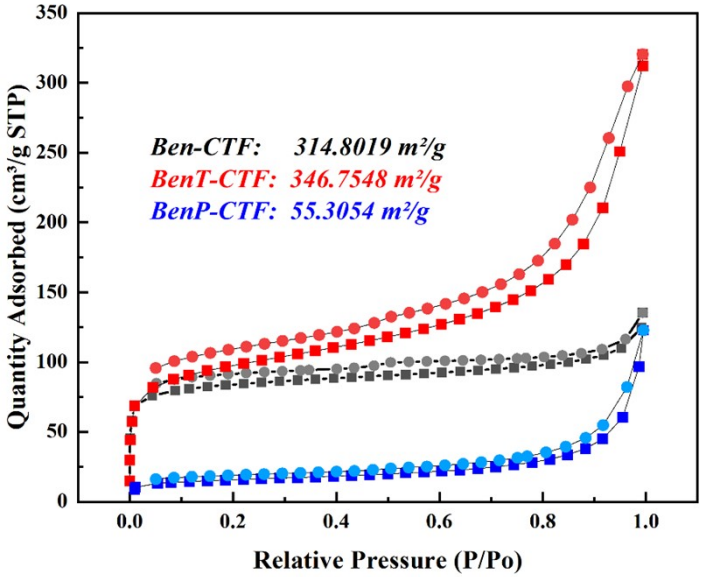

Figure S17. N_2 sorption isotherms of Ben-CTF, BenT-CTF and BenP-CTF.

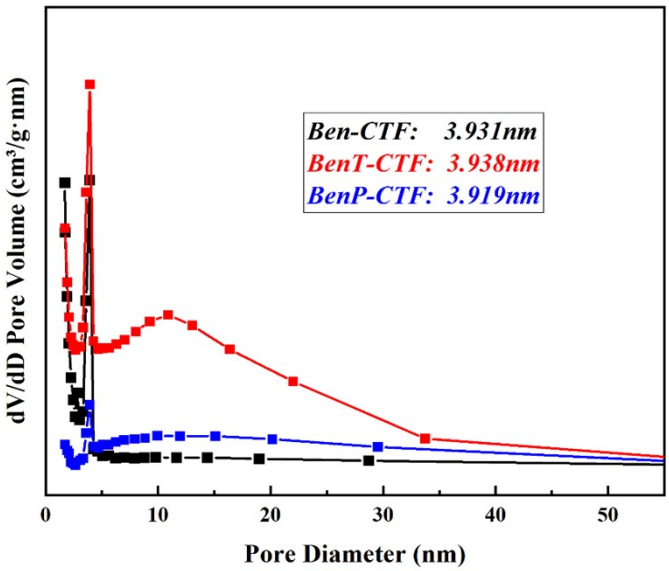

Figure S18. The corresponding pore size distribution of Ben-CTF, BenT-CTF and BenP-CTF.

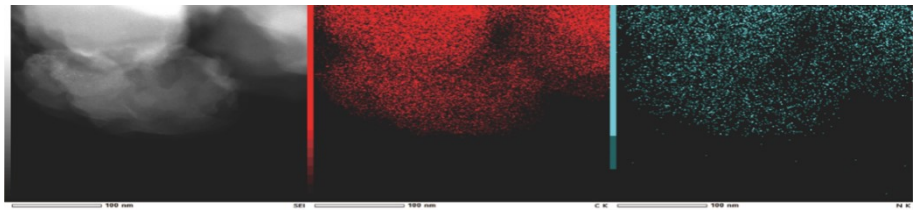

Figure S19. EDS images of Ben-CTF. Red and bule respectively represent the two elements of C, N.

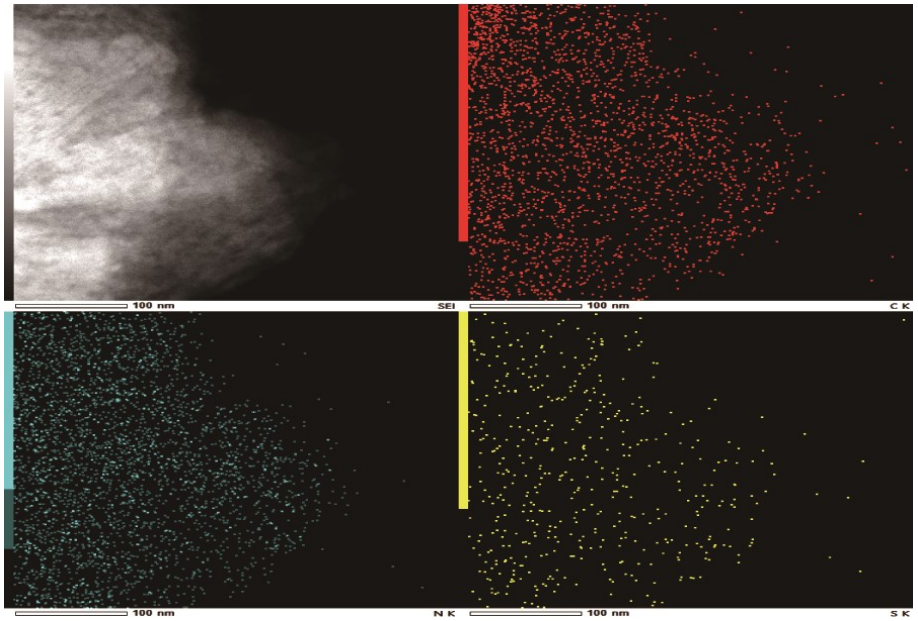

Figure S20. EDS images of BenT-CTF. Red, bule and yellow respectively represent the four elements of C, N, S.

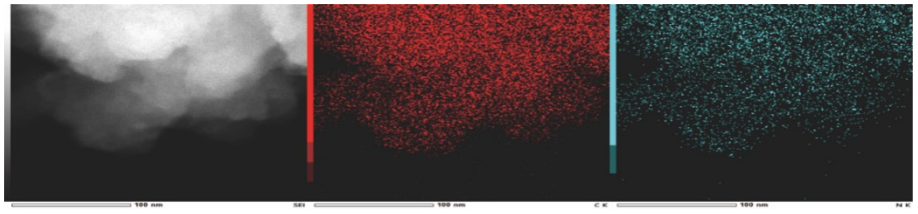

Figure S21. EDS images of BenP-CTF. Red and bule respectively represent the two elements of C, N.

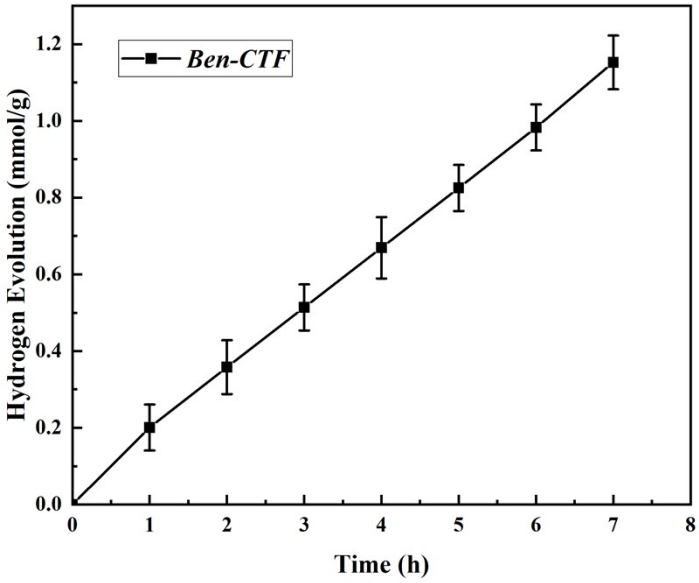

Figure S22. The photocatalytic hydrogen evolution performance of Ben-CTF.

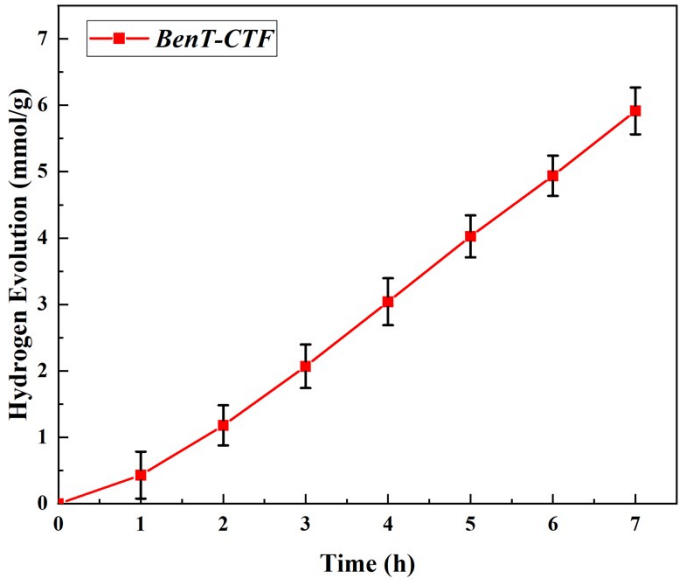

Figure S23. The photocatalytic hydrogen evolution performance of BenT-CTF.

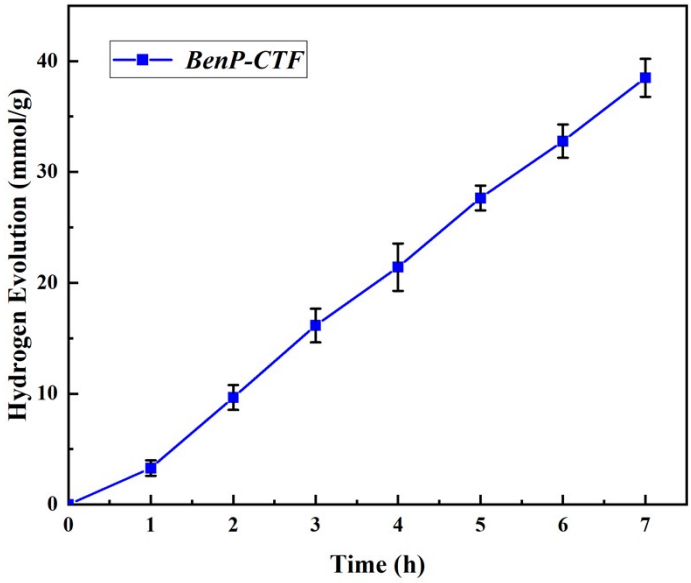

Figure S24. The photocatalytic hydrogen evolution performance of BenT-CTF.

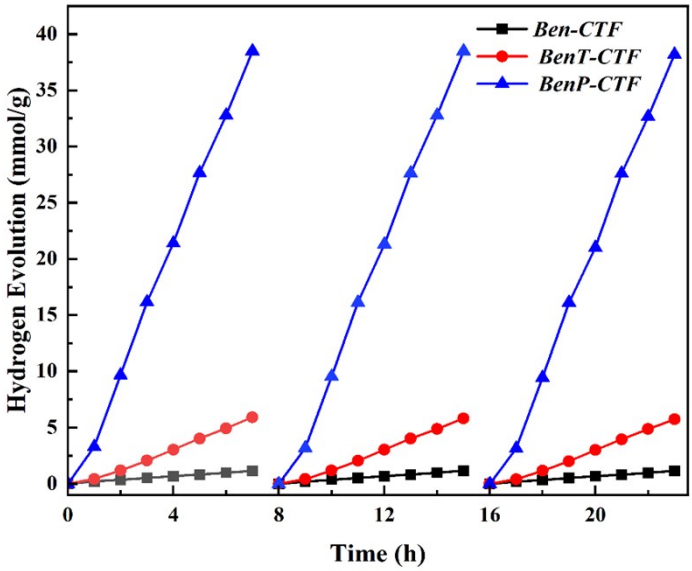

Figure S25. The cyclic hydrogen evolution performance of Ben-CTF, BenT-CTF and BenP-CTF.

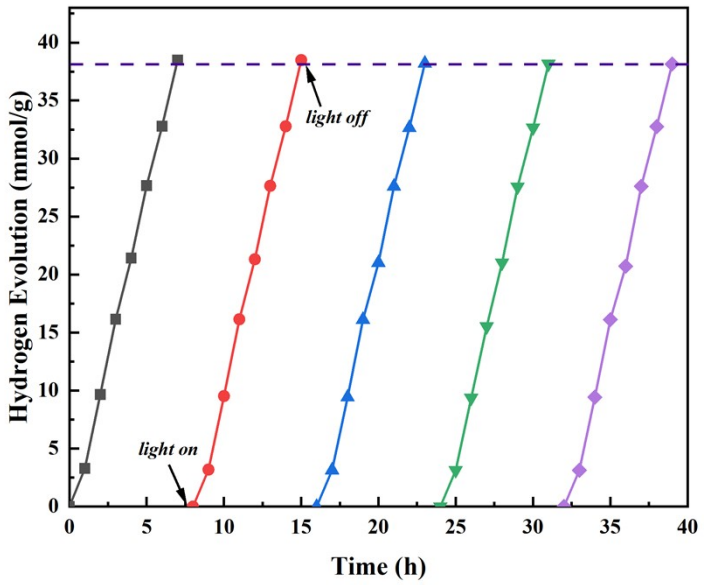

Figure S26. The further cyclic hydrogen evolution performance of BenP-CTF.

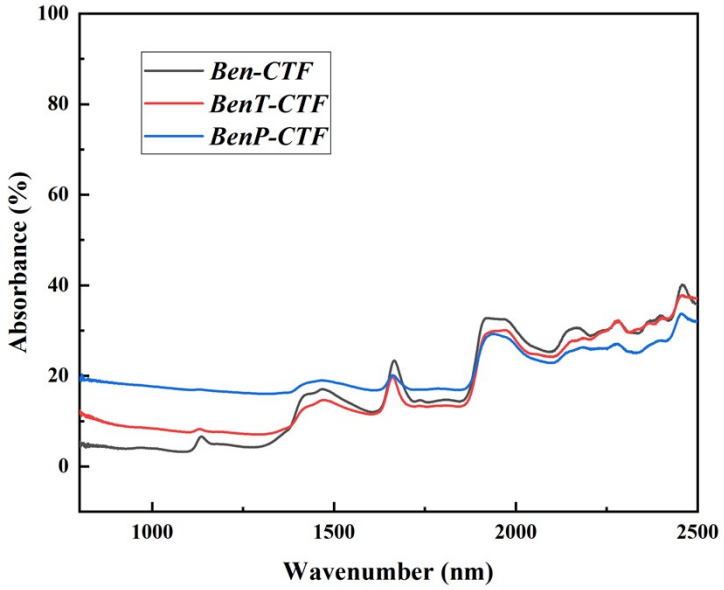

Figure S27. UV absorption spectra of three CTFs in the NIR region

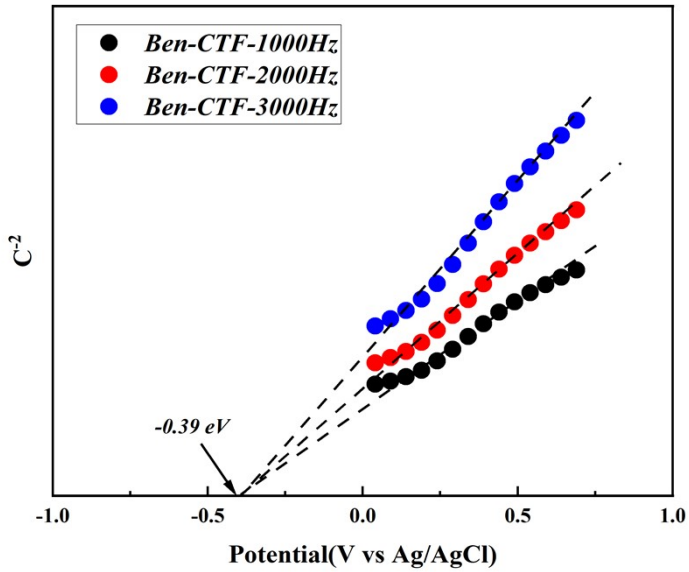

Figure S28. Mott-Schottky test chart for Ben-CTF.

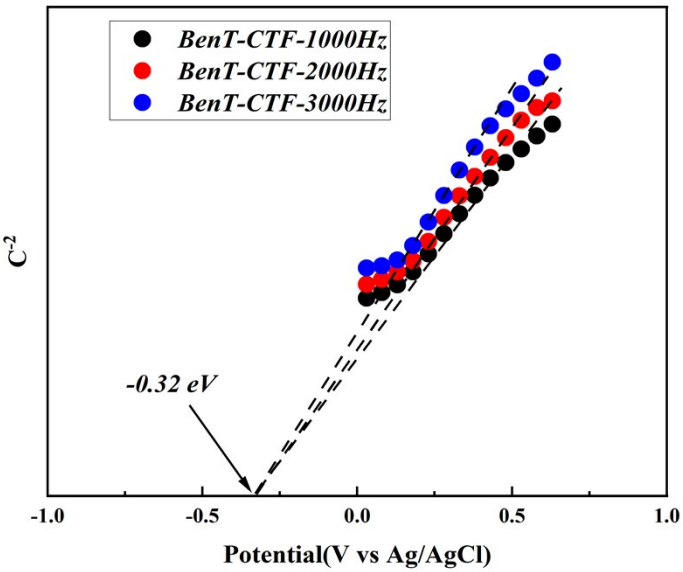

Figure S29. Mott-Schottky test chart for BenT-CTF.

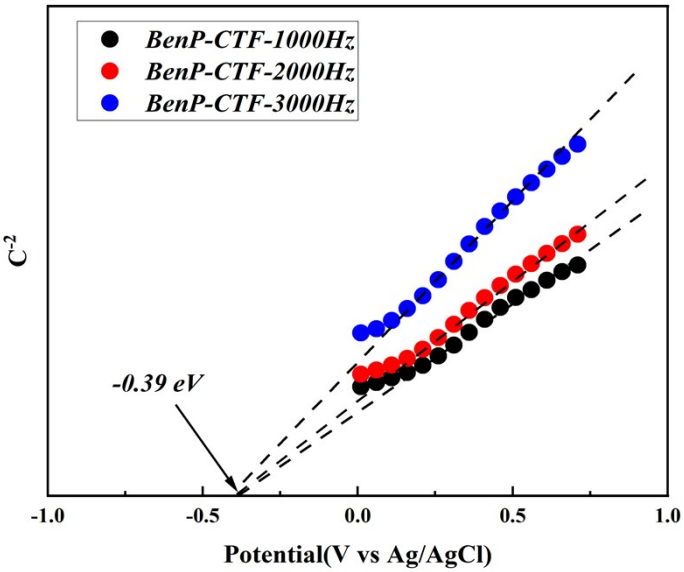

Figure S30. Mott-Schottky test chart for BenP-CTF.

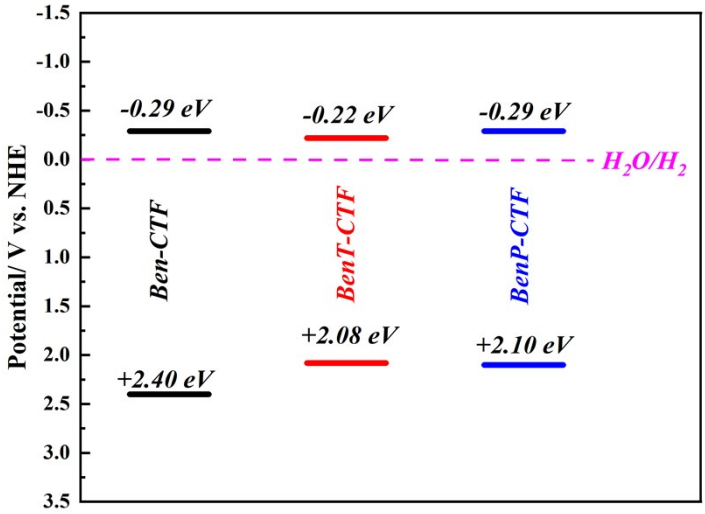

Figure S31. Energy band diagram of Ben-CTF, BenT-CTF, and BenP-CTF.

The method of calculating the band gap as follow equation:

$(\alpha hv)1/n = A(hv - Eg)$

α is the absorbance index, h is Planck's constant, v is the frequency, Eg is the forbidden bandwidth of the semiconductor, and A is a constant. n is related to the type of semiconductor, and n is taken as 1/2 in the case of direct bandgap semiconductors, and n is 2 in the case of indirect bandgap semiconductors.

CTFs is the direct bandgap semiconductor, and thus n is 1/2.

Table S1. Comparison of the photocatalytic H_2 generation performance of CTFs.

Photocatalysts	Condition	HER(μmol/h)	Ref
DV-Ti-3O	AM 1.5, MeOH, ~3 wt% Pt, 20mg	248.4	[2]
CTFS-1-10	>420 nm, TEOA，~3 wt% Pt, 50mg	249.6(S)	[3]
CTFSe-1-10		289.64(Se)	
CTF-HUST-S3	>420 nm, TEOA，~3 wt% Pt, 50mg	791	[4]
CTFS10	>420 nm, TEOA，~1 wt% Pt, 20mg	40	[5]
CTF-HUST-2	>420 nm, TEOA，~3 wt% Pt, 50mg	132.35	[6]
Ben-CTF (This work)	1.5G, TEOA，~3 wt% Pt, 50mg	13.7	This work
BenT-CTF (This work)	1.5G, TEOA，~3 wt% Pt, 50mg	24.5	This work
BenP-CTF (This work)	1.5G, TEOA，~3 wt% Pt, 50mg	332.5	This work

References

1. Giraldi, E., et al., *Metal-Stabilized Boronate Ester Cages.* Inorg Chem, 2021. **60**(15): p. 10873-10879.
2. Liu, S., et al., *The Role of Dual Vacancies in TiO2 for Enhanced Photocatalytic Hydrogen Generation and Pollutants Removal.* ChemCatChem, 2022. **14**(24): p. e202201107.

3. Chen, M., et al., *In-situ doping strategy for improving the photocatalytic hydrogen evolution performance of covalent triazine frameworks.* Science China Chemistry, 2023. **66**(8): p. 2363-2370.
4. Guo, L., et al., *Crystallization of Covalent Triazine Frameworks via a Heterogeneous Nucleation Approach for Efficient Photocatalytic Applications.* Chemistry of Materials, 2021. **33**(6): p. 1994-2003.
5. Li, L., et al., *Sulfur-doped covalent triazine-based frameworks for enhanced photocatalytic hydrogen evolution from water under visible light.* Journal of Materials Chemistry A, 2016. **4**(32): p. 12402-12406.
6. Wang, K., et al., *Covalent Triazine Frameworks via a Low-Temperature Polycondensation Approach.* Angew Chem Int Ed Engl, 2017. **56**(45): p. 14149-14153.